

Supporting Information

Chirality from scratch: enantioselective adsorption in geometrically controlled lateral nanoconfinement

Johannes Seibel¹, Zeno Tessari,¹ David B. Amabilino² and Steven De Feyter¹

¹ *Division of Molecular Imaging and Photonics, Department of Chemistry, KU Leuven, Celestijnenlaan 200F, 3001 Leuven, Belgium*

² *School of Chemistry & The GSK Carbon Neutral Laboratories for Sustainable Chemistry, The University of Nottingham, Triumph Road, Nottingham NG7-2TU, UK*

Corresponding authors: johannes.seibel@kuleuven.be, steven.defeyter@kuleuven.be

S1.	Experimental details.....	S2
S2.	Enantiopure BFA on pristine HOPG	S3
S3.	Statistics from individual sessions	S4
S4.	Rectangular nanocorrals and slower shaving speed.....	S5
S5.	Gel formation at higher concentrations.....	S6
S6.	Empty nanocorrals and contaminations	S6
S7.	Polymorph formation of enantiopure BFA	S7
S8.	Tentative model of intermolecular interactions in nanocorrals	S8

S1. Experimental details.

Chemicals

4-[(*S/R*-1-methylheptyl)oxy]-4'-biphenylform-amide (*S/R*-BFA) was synthesized according to a previously reported method.^[1] All other chemicals are commercially available and were used without further purification.

Scanning tunnelling microscopy (STM) and nanoshaving

All STM experiments were performed with PicoLE (Keysight) system operating in constant current mode at room temperature (20-22 °C). The STM tips used were mechanically cut from a Pt/Ir wire (80%/20%, 0.25 mm diameter). Small amounts of BFA solutions in 1-phenyloctane (Acros Organics, 99%) were dropcasted onto freshly cleaved or covalently modified highly oriented pyrolytic graphite (HOPG, grade ZYB, Advanced Ceramics Inc., Cleveland, OH, USA). All STM images were processed with the Scanning Probe Imaging Processor software (SPIP, Image Metrology ApS). Imaging parameters are indicated in the figure captions as V_b for the bias applied to the sample and I_t for tunnelling current.

Nanoshaving experiments were performed with CM-HOPG using the PicoLITH v2.1 software. All nanoshaving experiments were carried out with a sample bias of $V_b = -0.001$ V, tunnelling current setpoint $I_t = 200$ pA and a tip moving speed of 10 $\mu\text{m/s}$, except the “slow speed” experiments in figure S3, where the tip speed was 0.4 $\mu\text{m/s}$. The fast shaving direction was always parallel to the top border of each nanocorral. Immediately after the nanoshaving process, the nanocorrals were imaged.

Covalent modification of HOPG

Before each modification, HOPG was freshly cleaved using scotch tape. The electrochemical measurements were carried out with an Autolab PGSTAT101 (Metrohm Autolab BV, The Netherlands) in a home-built single compartment electrochemical cell with HOPG as the working electrode, a Pt wire counter electrode and an Ag/AgCl/ 3 M NaCl reference electrode. For the covalent modification of HOPG, 3,5-bis-*tert*-butylbenzenediazonium was synthesized *in-situ* from 3,5-bis-*tert*-butylaniline (TCI - Tokyo Chemical Industry Co., Ltd., 98%) by adding 100 μL of an aqueous NaNO_2 solution to 5mL of a 3 mM solution of the aniline in 50 mM HCl (aq.). Two minutes after the addition of NaNO_2 , the mixture was added to the electrochemical cell and three cycles between 0.6 V and -0.35 V were applied with a scan rate of 0.1 V/s. After the modification, the samples were rinsed with Milli-Q water (Milli-Q, Millipore, 18.2 M Ω) and Ethanol to remove physisorbed material and dried under Argon.

S2. Enantiopure BFA on pristine HOPG.

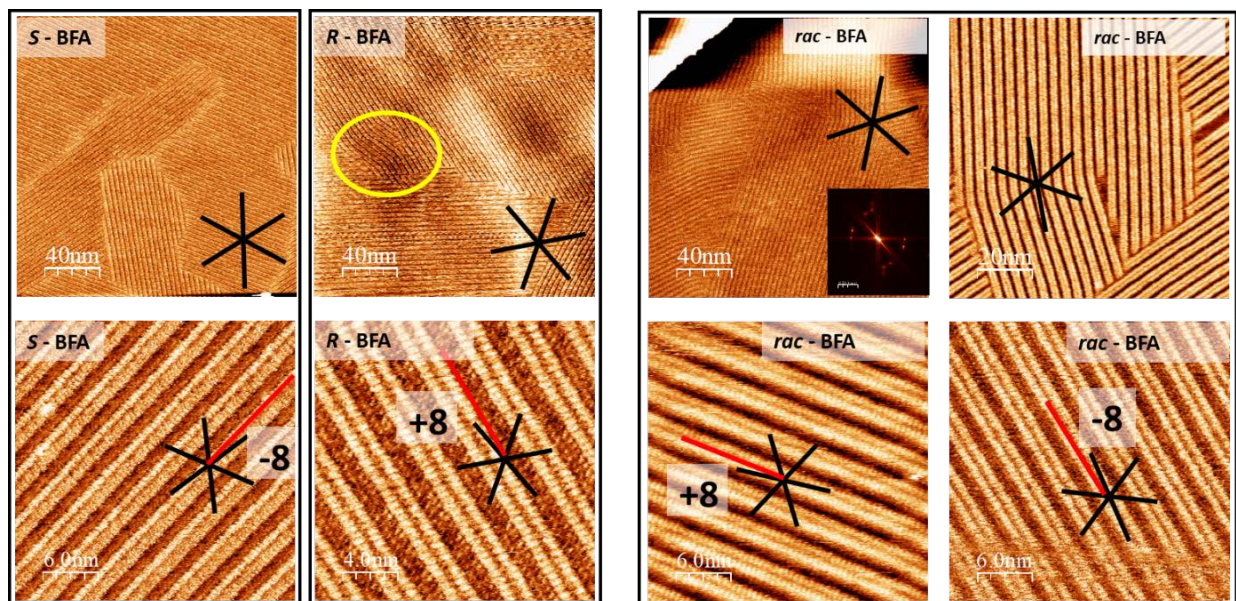


Figure S1. Representative large scale and high-resolution STM images of enantiopure (left) and racemic (right) BFA (15 mM in 1-phenyloctane) on pristine HOPG. The orientations and STM contrast of the domains found with the racemate correspond to either one of the enantiopure domains, indicating conglomerate formation. The yellow circle in the image of *R*-BFA marks an area with the orientation of *S*-BFA domains, which is most likely the result of small chiral impurities. Imaging parameters: $V_b = -0.7$ V, $I_t = 70$ pA.

Unit cell parameters:

R-BFA: $a = 0.60 \pm 0.02$ nm, $b = 3.99 \pm 0.06$ nm, $\alpha = 91.7^\circ \pm 2.0^\circ$, HOPG/row angle: $+7.8^\circ \pm 1^\circ$

S-BFA: $a = 0.60 \pm 0.02$ nm, $b = 3.94 \pm 0.15$ nm, $\alpha = 91.4^\circ \pm 1.0^\circ$, HOPG/row angle: $-7.5^\circ \pm 1.6^\circ$

Rac-BFA (*R* domain): $a = 0.59 \pm 0.02$ nm, $b = 4.06 \pm 0.06$ nm, $\alpha = 91.0^\circ \pm 1.4^\circ$, HOPG/row angle: $+8.2^\circ \pm 1^\circ$

Rac-BFA (*S* domain): $a = 0.60 \pm 0.02$ nm, $b = 3.98 \pm 0.02$ nm, $\alpha = 91.0^\circ \pm 0.9^\circ$, HOPG/row angle: $-7.0^\circ \pm 1^\circ$

S3. Statistics from individual sessions

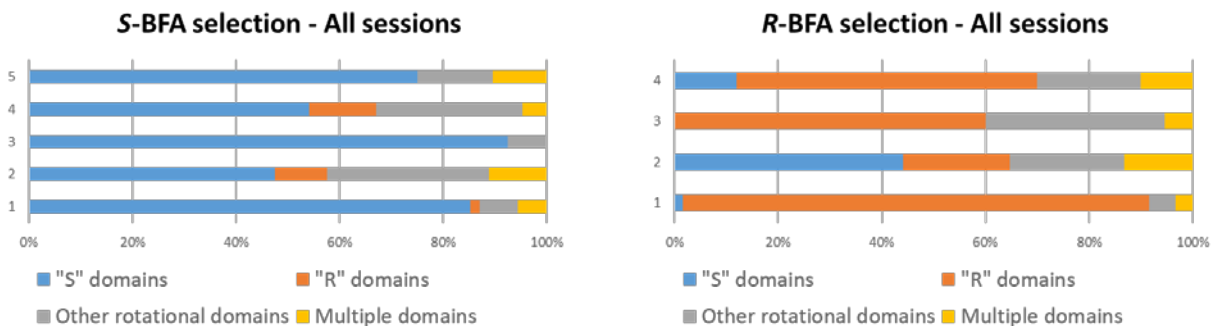


Figure S2. Statistics of all measurements sessions, which are summarized in the main text figure 2. The selection of the targeted enantiomer was found to differ between sessions, ranging between 50% and up to about 90%, with the exception of session 2 in the *R*-BFA selection. Additionally, the amount of rotational domains varied between sessions. A session is defined as all measurements carried out with the same sample as well as STM tip. For domain assignment see main text figure 2. Note that the number of nanocorrals measured is also different from session-to-session due to time restraints or changes in the STM tip conditions. Nanocorrals in *S*-BFA sessions 1-5: 54, 99, 80, 87, 48. Nanocorrals in *R*-BFA sessions 1-4: 60, 68, 75, 50.

S4. Rectangular nanocorrals and slower shaving speed

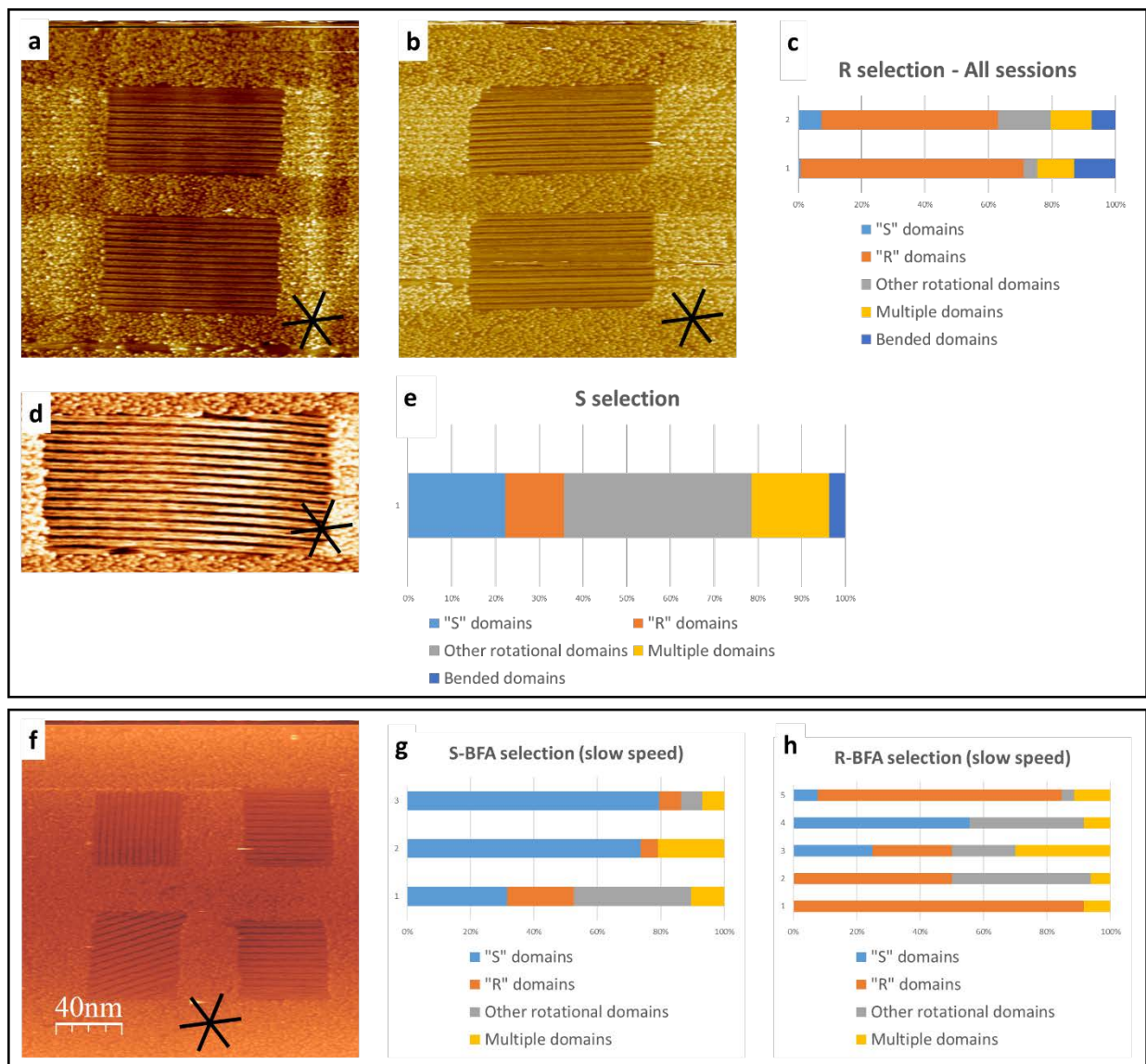


Figure S3. Representative STM images showing rectangular shaped nanocorrals with a size of approximately 100 nm x 50 nm (a and b). In these rectangular nanocorrals, occasionally bend rows were observed (d), which was not the case in the square shaped nanocorrals. However, the session-to-session variance was similar compared to the square shaped nanocorrals (c and e). Note that the number of nanocorrals measured is also different from session-to-session due to time restraints or changes in the STM tip conditions. Nanocorrals in rectangular S-BFA session: 141. Nanocorrals in rectangular R-BFA sessions 1 and 2: 138, 60.

The domain distributions statistics in nanocorrals produced with a slower shaving speed (0.4 $\mu\text{m/s}$) show a similar variance from session-to-session (g and h). A representative STM image with slow-shaving nanocorrals is shown in f. Nanocorrals in slow R-BFA sessions 1-5: 12, 16, 20, 36, 26. Nanocorrals in slow S-BFA sessions 1-3: 19, 19, 44.

Imaging parameters: $V_b = -0.7$ V, $I_t = 70$ pA, scan size: 200 nm x 200 nm (a, b and i), 120 nm x 60 nm (c).

S5. Gel formation at higher concentrations



Figure S4. Photographs showing the gel formation at room temperature (20-22 °C) of the solution when the concentration of *rac*-BFA is increased to 18 mM in 1-phenyloctane.

S6. Empty nanocorrals and contaminations

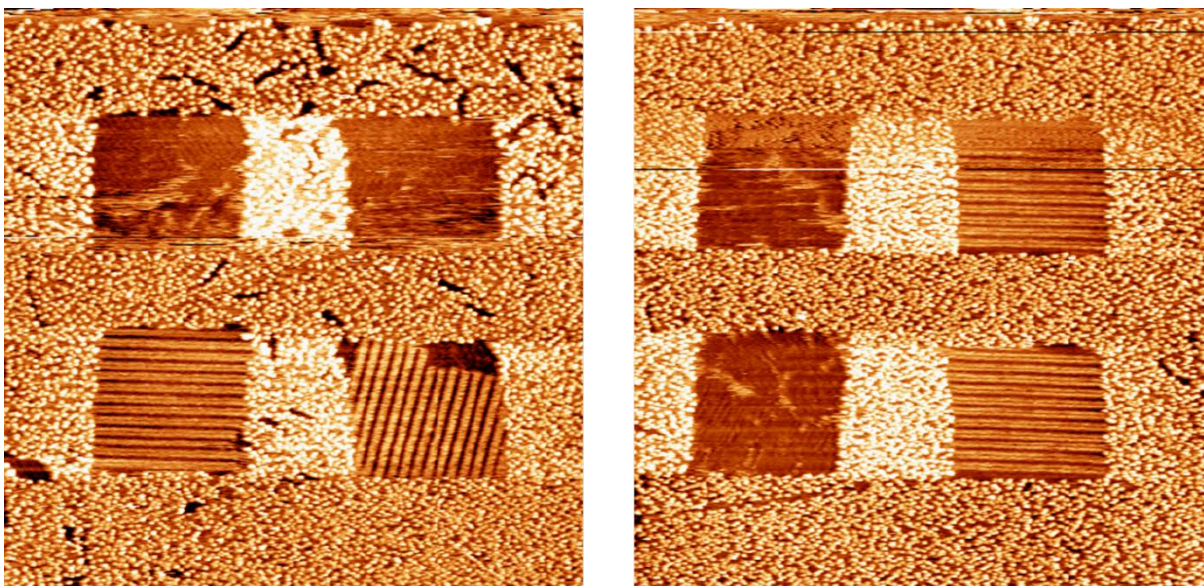


Figure S5. Representative STM images showing partially or completely empty nanocorrals containing some contaminations. These nanocorrals were not included in the domain distribution statistics. Imaging parameters: $V_b = -0.7$ V, $I_t = 70$ pA, scan size: 200 nm \times 200 nm.

S7. Polymorph formation of enantiopure BFA

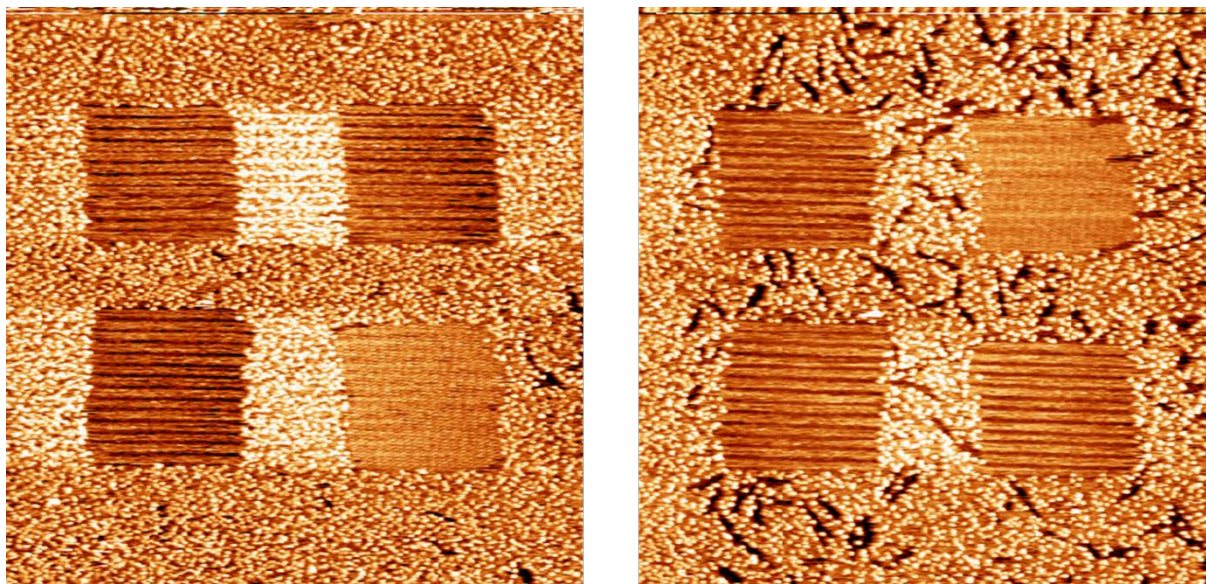


Figure S6. Representative STM images showing the occasional formation of the polymorph which usually observed when using lower concentrations (below 10 mM instead of 15 mM).^[2]

Imaging parameters: $V_b = -0.7$ V, $I_t = 70$ pA, scan size: 200 nm \times 200 nm.

S8. Tentative model of intermolecular interactions in nanocorrals

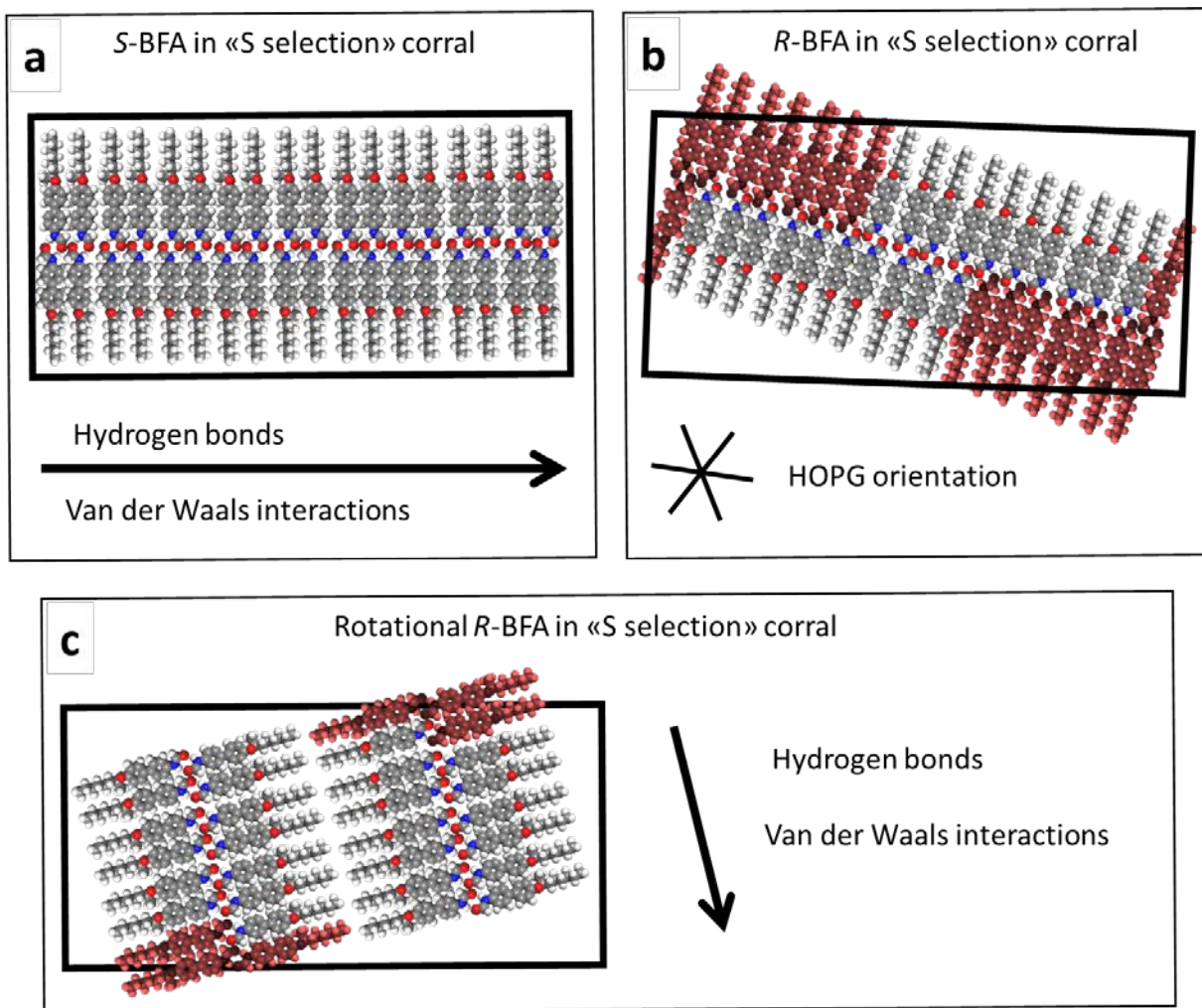


Figure S7. Tentative molecular model showing schematically the molecular alignment in nanocorrals during the initial stages of nanocorral formation, *i.e.* when the corral has a long aspect ratio, for the targeted enantiomer (a), the mirror domain (b) and a rotational domain (c). In the self-assembled row-structure of BFA, intermolecular interactions are predominantly along the row propagation direction in the form of hydrogen bonds and van-der-Waals interactions. These interactions are maximized in the assembly of S-BFA in the “S selection” nanocorral, *i.e.* when a row can align with the long nanocorral border.

References

- [1] D. B. Amabilino, E. Ramos, J. L. Serrano, T. Sierra, J. Veciana, *Polymer* **2005**, *46*, 1507–1521.
- [2] J. Seibel, D. B. Amabilino, S. De Feyter, *Angew. Chemie Int. Ed.* **2019**, *58*, 12964–12968.